Nanofabrication of Broad-Band Antireflective Surfaces Using Self-Assembly of Block Copolymers

Birgit Päivänranta,[†] Pratap K. Sahoo,[†,⊥] Elizabeth Tocce,[‡] Vaida Auzelyte,[†] Yasin Ekinci,[†,§] Harun H. Solak,[†] Chi-Chun Liu,[‡] Karl O. Stuen,[‡] Paul F. Nealey,[‡] and Christian David[†,*]

[†]Laboratory for Micro- and Nanotechnology, Paul Scherrer Institut, CH-5232 Villigen-PSI, Switzerland, [‡]Department of Chemical and Biological Engineering, University of Wisconsin, Madison, Wisconsin 53706-1691, United States, and [§]Laboratory of Metal Physics and Technology, Department of Materials, ETH Zurich, 8093 Zurich, Switzerland. [⊥] Present address: National Institute of Science Education and Research (NISER), Bhubaneswar-751005, Orissa, India.

ABSTRACT We present a simple and cost-effective method for the fabrication of antireflective surfaces by self-assembly of block copolymers and subsequent plasma etching. The block copolymers create randomly oriented periodic patterns, which are further transferred into fused silica substrates. The reflection on the patterned fused silica surface is reduced to well below 1% in the ultraviolet, visible, and near-infrared ranges by exploiting subwavelength nanostructures with periodicities down to 48 nm. We show that by choosing the appropriate block copolymers and pattern transfer parameters the optical properties of the antireflective surface can be easily tuned, and the spectral measurements verify a significant reduction of the reflectivity by a factor of 10. The experiments, confirmed with simulations based on rigorous diffraction theory, also show that the tapered shape of the nanostructures gives rise to a graded index surface, resulting in a broad-band antireflective behavior.

KEYWORDS: antireflection · block copolymers · nanofabrication · subwavelength gratings · broad-band

Suppression of reflection of light at the interfaces of dielectric media is of critical importance in many applications. Light reflection from the surfaces of transparent optical elements such as lenses, solar cells, detectors, and displays can significantly deteriorate the optical performance of the device by causing stray light or by reducing the efficiency. Therefore, optical surfaces are often covered with antireflective (AR) layers in order to eliminate or reduce reflection while enhancing the transmission. Mostly these surfaces consist of vacuum-deposited dielectric coatings whose functional principle is based on thin film interference, and thereby reduce the intensity of the reflected wave. However, this technique has a number of severe drawbacks. First, in order to achieve well-defined broad-band AR properties over oblique incident angles, a large number of thin film layers have to be applied with high precision, which can become too costly for some applications.[1] In addition, obtaining dielectric AR coatings is challenging in the ultraviolet (UV) range, as the choice of suitable coating materials with sufficiently low absorption becomes very limited. Moreover, when used with high-power lasers, the fragility of AR coatings can severely restrict their use. A potential alternative to dielectric coatings that can address some of these limitations is provided by subwavelength surface gratings. This approach is highly nature-inspired, thus these types of periodic surface relief structures were originally discovered on the cornea of night-flying moths by Bernhard.[2] Since then, patterning subwavelength grating structures[3−10] has attracted substantial interest as a powerful method for obtaining AR properties. Oblique incidence thin film deposition methods,[1] replicated polymer structures,[2,3,11−13] tailored silicon surfaces,[14−16] etched fused silica and glass surfaces,[7,8,12] carbon nanotube arrays,[9] and nanoporous polymers[10,17] have been utilized for obtaining optical surfaces with AR properties.

While there are similarities in how the nanostructured and dielectric film-coated surfaces lead to reduced reflection, nanostructured surfaces open up new dimensions of parameters that are not readily available in dielectric coatings. According to scalar diffraction theory, the reflectivity of a substrate covered with a thin dielectric layer is eliminated when the two interfaces generate two reflected waves of (i) equal amplitude and (ii) opposite phase. According to the well-known Fresnel formulas, the reflectivity of a layer is determined by matching the refractive index ratios on both interfaces of the thin film (see Figure 1). This leads to the AR criterion $n_1 = (n_0 n_2)^{1/2}$,[18] where n_1, n_0,

*Address correspondence to christian.david@psi.ch.

Received for review December 7, 2010 and accepted February 4, 2011.

Published online February 16, 2011
10.1021/nn103361d

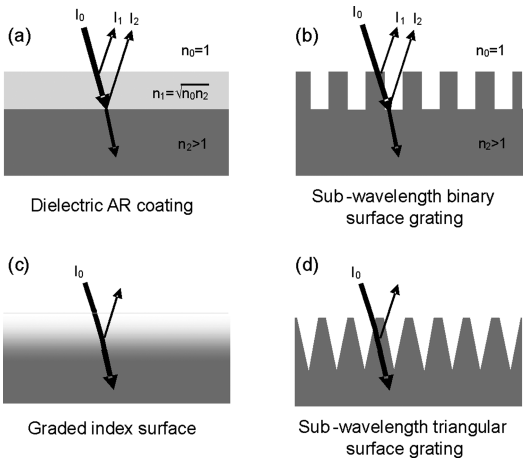

Figure 1. Schematic picture showing different methods for suppressing reflection from a surface. (a) Applying a coating layer, (b) structuring the surface with a binary shaped pattern, (c) obtaining a graded index surface without sharp interfaces, and (d) structuring the surface for obtaining graded index modulation.

and n_2 are the refractive indices of the AR thin film and media in the incident and transmission sides, respectively, which satisfies the first condition. In the case of a normal incidence, the second condition is fulfilled when a layer thickness d is equal to a quarter of the light wavelength inside the dielectric coating layer, $d = \lambda/4n_1$, where λ is the wavelength.

A grating on a surface can be used to obtain an arbitrary refractive index formed in the modified grating region by engineering the geometry of the grating structures. For a subwavelength grating period, $p < \lambda/(n_2 + n_0|\sin\theta|)$, where θ is the incident angle, there are no propagating diffraction channels, but the grating can still significantly harness the intensity, phase, and polarization of the transmitted and the reflected waves.[19] For a binary grating shown in Figure 1b, the effective refractive index, n_{eff}, is given by the formula $n_{eff} = (n_1 - 1)DC + 1$, where the duty cycle DC is defined as the ratio of the dielectric grating line with a width w to the grating period p. When the surrounding medium is air and the grating is of the same material as the substrate, the optimum duty cycle in terms of the AR criterion is $DC = (\sqrt{n_2} - 1)/(n_2 - 1)$. For example, when considering glass materials with refractive index values of approximately 1.5, one can calculate the optimal DC to be 0.45. This type of binary subwavelength grating basically exhibits the same spectral response as a single-layer dielectric AR coating. Alas, in both of these cases, the AR functionality is achieved only over a narrow wavelength range. However, the wavelength range can be broadened by varying the refractive index to continuously change between the two surrounding media (see Figure 1c). Performance of such graded index surfaces with more profound AR properties has been investigated by Lowdermilk.[8] The analogous AR grating structure would need to have a continuous change in n_{eff}, meaning that DC should continuously change along the depth of the grating lines, which can be achieved by tapered line profiles (see Figure 1d). An optimal subwavelength structured AR surface would consist of randomly oriented subwavelength gratings having tapered structure profiles. When the subwavelength grating is made from the same material as the substrate, the index matching at the substrate interfaces can lead to highly improved AR performance.[12,20,21]

Applying purely lithographic techniques for fabrication of the randomly oriented graded index structures is challenging and expensive, in particular, over large areas and on curved surfaces. Furthermore, according to the subwavelength criteria, an AR surface suitable for UV range has to have a grating period of 100 nm or smaller. In terms of usual lithographic resolution specifications, this is only available through advanced methods such as electron beam, deep-UV, or extreme UV interference lithography.[22] Nanopatterning using self-assembled block copolymer (BC) structures offers an ideal solution for high-resolution patterning due to its ability to produce ordered nanostructures over large areas with periodicities in the relevant range.[23,24] Block copolymers can form grating structures inexpensively and with high throughput, which makes the technique attractive for manufacturing AR surfaces for a wide variety of applications. In this paper, we present a simple and efficient method for producing highly periodic graded index subwavelength nanostructures with highly efficient and broad-band AR properties from near-infrared (NIR) to UV ranges.

RESULTS AND DISCUSSION

Block copolymer patterns consisting of polystyrene (PS) and polymethyl methacrylate (PMMA) with varying periodicities were fabricated on fused silica (FS) substrates by self-assembly and by choosing different copolymer blends for obtaining different periodicities. By selective removal of the PMMA by oxygen plasma etching,[26] self-assembled 35 nm thick PS mask layers with three different grating periods of 48, 76, and 100 nm were obtained on the substrates. Figure 2a shows a typical scanning electron microscope (SEM) image of the 48 nm period PS structure on a FS substrate before the pattern transfer. Even though the structures are randomly oriented, they exhibit a high degree of periodicity. For the study of AR properties, the PS pattern was transferred into the FS substrate by using two plasma etching steps, which are shown in Figure 3. This process results in a purely dielectric AR nanostructure area over the FS substrate. Figure 2b shows a cross-sectional SEM image of 100 nm period FS nanostructures with a side wall angle of around 12°, which is typical for our FS etching process. The depth of the

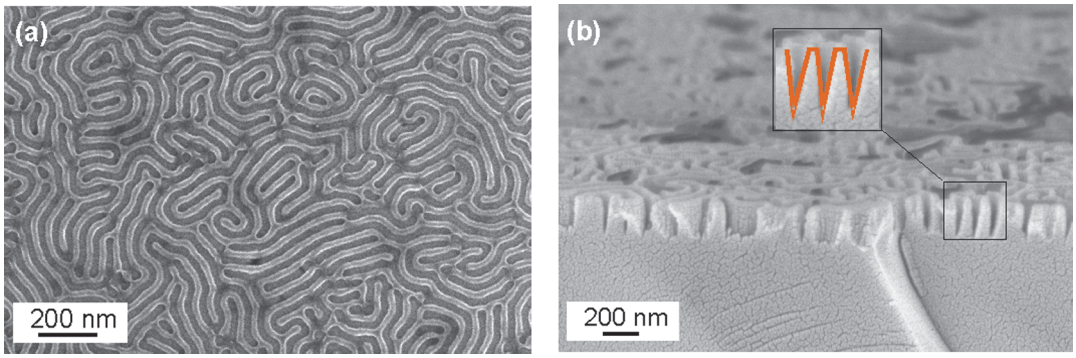

Figure 2. SEM images of (a) the PS structures with a 48 nm period after selective removal of PMMA and (b) a cross section of 100 nm period structures etched deep into fused silica for 720 s.

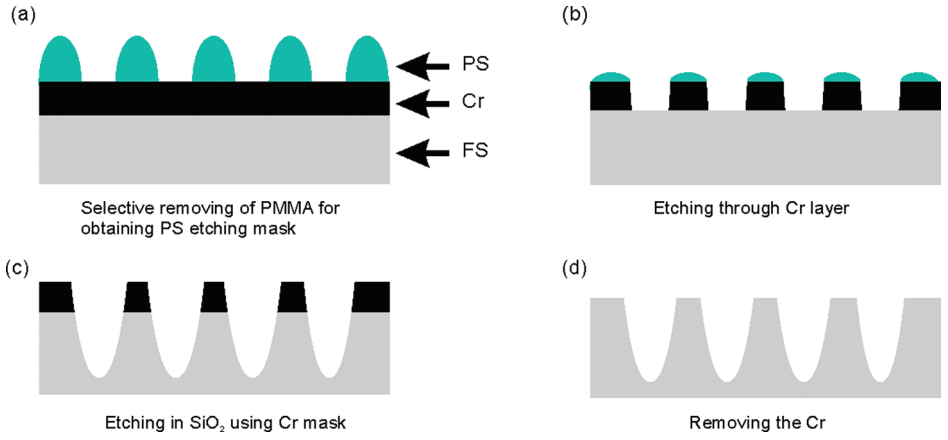

Figure 3. Fabrication process for transferring the PMMA–PS block copolymer AR structure into fused silica (FS). (a) After selective removal of PMMA, (b) the PS is used as an etching mask in chlorine-based plasma etching to penetrate Cr, after which (c) the Cr is used as an etching mask to transfer the pattern into FS by fluorine-based plasma etching, and (d) the Cr is removed by wet etching.

structures is controlled by the FS etching time. However, because of the side wall angle, the maximum depth that can be achieved is limited by the period.

We investigated the reflectivity of FS substrates structured with three types of AR nanopatterns having periodicities of 48, 76, and 100 nm by using spectroscopic measurements. The reflectance spectra over the UV–NIR wavelength range for AR patterns with different etching times and with 100 nm period as well as for unpatterned substrate surface are shown in Figure 4. Over this measured range, the unpatterned FS is known to reflect around 4% of the incident light.[18] After modifying the surface with the nanostructure, the reflectivity of the FS surface is reduced over a broad wavelength range by a factor of 10, resulting in reflectivities below 1%. With the longest etching time, the reflectance spectrum exhibits a minimum at a wavelength of approximately 500 nm. When the etching time is decreased, the dip in the reflectivity spectra is systematically blue-shifted due to the reduced nanostructure height in accordance with the aforementioned thin film interference theory.

Also, depending on the structure profile, the wavelength range showing the strongest suppression of

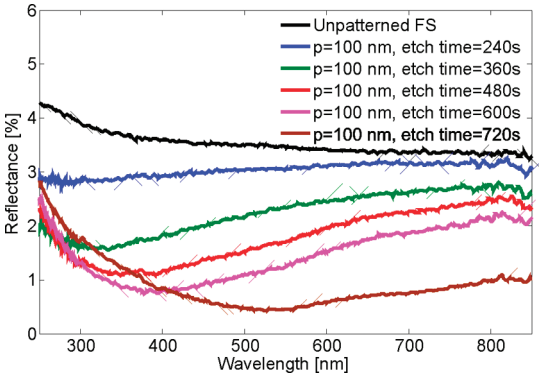

Figure 4. Experimental reflectance spectra of unpatterned and patterned fused silica (FS) surfaces for a 100 nm period nanostructure for various fused silica (FS) etching times.

reflection can be varied, as shown in Figure 5. The AR wavelength range can be tuned by choosing the optimal BC period. In addition, the best structure profile leading to the lowest broad-band reflection for a given period is obtained by finding the FS etching time producing the tapered side wall angle with an optimal depth. For our structures, this was reached by varying the etching time between 6 and 12 min, depending on the period. With etching times of 720,

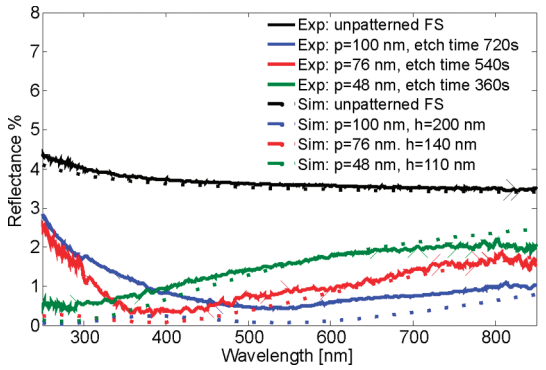

Figure 5. Experimental reflectance curves and comparison to rigorous simulations for periods of 100, 76, and 48 nm. The structures with higher periods (100 and 76 nm) have well-defined antireflection properties over the visible wavelength range, whereas the 48 nm period significantly reduces the reflection at the UV range.

540, and 360 s for periods of 100, 76, and 48 nm, respectively, we obtained reflectance minima at approximately 550, 380, and 280 nm, respectively (see Figure 5).

For a better understanding of the AR properties, theoretical analysis based on widely used rigorous diffraction theory (*i.e.*, Fourier modal method)[19] was performed. In order to simplify the simulations, a normal incidence illumination and a linear multilayer grating profile were assumed. The average of the intensities of transverse electric (TE) and transverse magnetic (TM) modes was taken in order to reach an approximation for unpolarized light. For antireflection surface illuminated at normal incidence, the difference between TE and TM is small but increases when the incident angle is increased.[12] The input/output media were assumed to be air, whereas the grating consisted of the substrate material. Since the present structures fulfill the subwavelength criteria for the wavelength range under consideration, the calculations were limited to the zeroth-order diffraction only.

As can be seen from the SEM image shown in Figure 2b, the AR surface obtained by BC patterning has the shape of a truncated triangle (T-triangle). Thus, in our simulations, a model of top-flatted triangles has been considered, where a 10% top truncation with respect to the period has been assumed. These calculations verify that the T-triangle grating profile shows a good match to our experimental results, as can be seen from Figure 5, where comparisons between experimental and simulation results for three grating periods are shown. We observe a significant reduction in the reflectance especially at the shorter wavelengths due to the gradual change of the effective refractive index in the modified grating region. Further optimization of the T-triangle profile can lead to even more significant improvement of the antireflection behavior in the red and NIR regions. The mismatches between theory and experiments, especially for larger periods in wavelengths below 300 nm, may be explained by taking into account the random and varying periodicity and shape of the BC patterns (see Figure 2). The lower spatial frequencies in the surface pattern can cause diffuse scattering, meaning that, for very short wavelengths, parts of the structure dimensions are no longer truly subwavelength. The proposed surface would work as an antireflective one also for higher incidence angles, but due to the shallowness, the performance would not be optimal.[12] By using a more selective etching process, the pattern height could be increased and wide-angle performance obtained.

CONCLUSIONS

We have demonstrated a fabrication method for large-area subwavelength nanostructured fused silica surfaces with superior AR performance by exploiting the self-assembly of block copolymers. By selecting suitable block copolymer blends and optimized etching process, the periodicity, duty cycle, depth, and the profile of the nanostructures can be easily altered. With a nanostructure profile having a shape of a truncated triangle, the reflectance of fused silica was suppressed up to a factor of 10 in a broad wavelength range from NIR down to the deep-UV wavelengths. The rigorous diffraction analysis confirmed that the broad-band AR behavior of the fabricated surfaces is governed by the triangular profile of the nanostructures. The continuous nanopattern profile is shown to be highly beneficial for antireflection performance because it gives rise to gradual change in effective refractive index in the modified grating region. On the basis of this principle, our calculations indicate that further optimization of the nanostructure profiles will lead to better AR properties in even a broader wavelength range. In addition, given the low periodicities of the fabricated nanostructures, they can clearly govern AR properties also at higher incident angles. The presented fabrication method offers a low-cost alternative to obtain AR surfaces and is particularly interesting for applications on curved surfaces or in the UV range as well as in applications where robustness against harsh environment or high light power is required.

METHODS

Subwavelength Pattern Fabrication. Block copolymer (BC) films were formed on 0.5 mm thick, 4 in. size high-purity fused silica (HPFS) wafers (Corning 7980, standard grade) covered by a 15 nm thick thermally evaporated Cr layer. First, a benzocyclobutene containing random copolymers of polystyrene (PS) and poly(methyl methacrylate) (PMMA)[25] (~2% benzocyclobutene, 56% polystyrene, 42% poly(methyl methacrylate)) was dissolved in

0.2 wt % toluene. The polymer was spun-cast onto the fused silica (FS) substrate at 4000 rpm. The sample was baked at 190 °C for 4 h to cross-link the film, and the un-cross-linked polymers were removed by sonication in toluene, resulting in an approximately 7 nm thick polymer mat. Next, block copolymer films were cast on the mat-coated substrate to yield films having a thickness of 30 nm. Each BC or BC blend was annealed at 190 °C for 24 h in order to yield lamellar domains oriented perpendicular to the substrate. Pure BCs of polystyrene-*block*-poly(methyl methacrylate) with the molecular weights of 50-*b*-54 kg/mol and 85-*b*-91 kg/mol were used to produce structures with periods of 48 and 72 nm, respectively. A blend of polystyrene-*block*-poly(methyl methacrylate) (85-*b*-91 kg/mol) with homopolymers of polystyrene (46 kg/mol) and poly(methyl methacrylate) (46 kg/mol) added in volume fractions of 0.7, 0.15, and 0.15, respectively, were used to create structures having 100 nm period.

By selective removal of PMMA, the PS structure was obtained which was used as an etching mask to penetrate through a 15 nm thick Cr layer by plasma etching in Cl_2/CO_2 plasma (100:100 sccm ratio and 280 mTorr). The etching time was varied from 30 to 50 s in order to fully remove the exposed chromium layer. Then, by using the Cr as a second mask, the nanopattern was further transferred into the FS by reactive ion etching in CHF_3/O_2 plasma (20:20 sccm ratio, 100 mTorr). The FS etching time was varied between 3 and 12 min in order to obtain structures with various depths with an etching speed between 13 and 16 nm/min. Finally, the residual Cr layer was removed by wet chemical etching.

Optical Characterization. The transmission spectra $T(\lambda)$ of the AR surfaces were measured over a wavelength range of 250−850 nm using a spectrometer from Perkin-Elmer (Lambda 9, UV/vis/NIR spectrometer) in a dual beam (sample and reference beam) configuration, and the nanostructured surface of the sample was oriented toward the light source. The reflection spectrum $R_1(\lambda)$ of the sample was determined from the transmission data using the relation $T(\lambda) = (1 - R_1(\lambda) - R_2(\lambda))$. The reflection spectrum $R_2(\lambda)$ of the unstructured exit side was obtained by measuring the transmission spectrum $T_0(\lambda)$ of an unpatterned region of the sample. As in these regions the reflectivity of both sides can be assumed to be equal, $R_2(\lambda)$ can be obtained from $T_0(\lambda) = (1 - 2R_2(\lambda))$. In all our analysis, we assume that diffuse scattering and absorption at the wavelength range under consideration is negligible.

REFERENCES AND NOTES

1. Xi, J. Q.; Schubert, M. F.; Kim, J. K.; Schubert, E. F.; Chen, M.; Lin, S.-Y.; Liu, W.; Smart, J. A. Optical Thin-Film Materials with Low Refractive Index for Broadband Elimination of Fresnel Reflection. *Nat. Photonics* **2007,** *1*, 176–179.
2. Bernhard, C. G. Structural and Functional Adaptation in a Visual System. *Endeavour* **1967,** *26*, 79–84.
3. Kanamori, Y.; Hane, K. Broadband Antireflection Subwavelength Gratings for Polymethyl Methacrylate Fabricated with Molding Technique. *Opt. Rev.* **2002,** *9*, 183–185.
4. Lee, C.; Bae, S. Y.; Mobasser, S.; Manohara, H. A Novel Silicon Nanotips Antireflection Surface for the Micro Sun Sensor. *Nano Lett.* **2005,** *5*, 2438–2442.
5. Lee, Y.-J.; Ruby, D. S.; Peters, D. W.; McKenzie, B. B.; Hsu, J. W. P. ZnO Nanostructures as Efficient Antireflection Layers in Solar Cells. *Nano Lett.* **2008,** *8*, 1501–1505.
6. Huang, Y.-F.; Chattopadhyay, S.; Jen, Y.-J.; Peng, C.-Y.; Liu, T.-A.; Hsu, Y.-K.; Pan, C.-L.; Lo, H.-C.; Hsu, C.-H.; Chang, Y.-H.; *et al.*Improved Broadband and Quasiomnidirectional Anti-Reflection Properties with Biomimetic Silicon Nanostructures. *Nat. Nanotechnol.* **2007,** *2*, 770–774.
7. Lohmüller, T.; Helgert, M.; Sundermann, M.; Brunner, R.; Spatz, J. P. Biomimetic Interfaces for High-Performance Optics in the Deep-UV Light Range. *Nano Lett.* **2008,** *8*, 1429–1433.
8. Lowdermilk, W. H.; Milam, D. Graded-Index Antireflection Surfaces for High-Power Laser Applications. *Appl. Phys. Lett.* **1980,** *36*, 891–893.
9. Yang, Z. P.; Ci, L.; Bur, J. A.; Lin, S. Y.; Ajayan, P. M. Experimental Observation of an Extremely Dark Material Made by a Low-Density Nanotube Array. *Nano Lett.* **2008,** *8*, 446–451.
10. Hiller, J. A.; Mendelsohn, J. D.; Rubner, M. F. Reversibly Erasable Nanoporous Anti-Reflection Coatings from Polyelectrolyte Multilayers. *Nat. Mater.* **2002,** *1*, 59–63.
11. David, C.; Häberling, P.; Schnieper, M.; Söchtig, J.; Zschokke, C. Nano-Structured Anti-Reflective Surfaces Replicated by Hot Embossing. *Microelectron. Eng.* **2002,** *61−62*, 435–440.
12. Päivänranta, B; Saastamoinen, T; Kuittinen, M. A Wide-Angle Antireflection Surface for the Visible Spectrum. *Nanotechnology* **2009,** *20*, 375301.
13. Yu, Z.; Gao, H.; Wu, W.; Ge, H.; Chou, S. Fabrication of Large Area Subwavelength Antireflection Structures on Si Using Trilayer Resist Nanoimprint Lithography and Liftoff. *J. Vac. Sci. Technol., B* **2003,** *21*, 2874–2877.
14. Kanamori, Y.; Hane, K.; Sai, H.; Yugami, H. 100 nm Period Silicon Antireflection Structures Fabricated Using a Porous Alumina Membrane Mask. *Appl. Phys. Lett.* **2001,** *78*, 142–143.
15. Striemer, C. C.; Fauchet, P. M. Dynamic Etching of Silicon for Broadband Antireflection Applications. *Appl. Phys. Lett.* **2002,** *81*, 2980–2982.
16. Chang, Y. C; Mei, G. H; Chang, T. W; Wang, T. J; Lin, D. Z; Lee, C. K Design and Fabrication of a Nanostructured Surface Combining Antireflective and Enhanced-Hydrophobic Effects. *Nanotechnology* **2007,** *18*, 285303.
17. Ibn-Elhaj, M.; Schadt, M. Optical Polymer Thin Films with Isotropic and Anisotropic Nano-Corrugated Surface Topologies. *Nature* **2001,** *410*, 796–799.
18. Born, M.: Wolf, E. Basic Properties of the Electromagnetic Field. *Principles of Optics*, 7th ed.; Cambridge University Press: Cambridge, UK, 2005; pp 64−70.
19. Turunen, J. In *Micro-Optics*; Herzig, H. P., Ed.; Taylor & Francis: London, 1998.
20. Ono, Y.; Kimura, Y.; Ohta, Y.; Nishida, N. Antireflection Effect in Ultrahigh Spatial-Frequency Holographic Relief Gratings. *Appl. Opt.* **1987,** *26*, 1142–1146.
21. Ichikawa, H Subwavelength Triangular Random Gratings. *J. Mod. Opt.* **2002,** *49*, 1893–1906.
22. Solak, H. H. Nanolithography with Coherent Extreme Ultraviolet Light. *J. Phys. D: Appl. Phys.* **2006,** *10*, R171–R188.
23. Ruiz, R.; Kang, H.; Detcheverry, F. A; Dobisz, E.; Kercher, D. S.; Albrecht, T. R.; de Pablo, J. J.; Nealey, P. F. Density Multiplication and Improved Lithography by Directed Block Copolymer Assembly. *Science* **2008,** *321*, 926–939.
24. Han, E.; Stuen, K. O.; La, Y.-H.; Nealey, P .F.; Gopalan, P. Effect of Composition of Substrate-Modifying Random Copolymers on the Orientation of Symmetric and Asymmetric Diblock Copolymer Domains. *Macromolecules* **2008,** *41*, 9090–9097.
25. Ryu, D. Y.; Shin, K.; Drockenmuller, E.; Hawker, C. J.; Russell, T. P. A Generalized Approach to the Modification of Solid Surfaces. *Science* **2005,** *308*, 236–239.
26. Liu, C.-C.; Nealey, P. F.; Ting, Y.-H.; Wendt, A. E. Pattern Transfer Using Poly(styrene-*block*-Methyl methacrylate) Copolymer Films and Reactive Ion Etching. *J. Vac. Sci. Technol., B* **2007,** *25*, 1963–1968.